Articles

Monomeric and Trimeric Manganese(III) Complexes of 2-Hydroxy-5,10,15,20-tetraphenylporphyrin. Synthesis and Characterization

Jacek Wojaczyński and Lechosław Latos-Grażyński*

Department of Chemistry, University of Wrocław, 14 F. Joliot-Curie Street, 50 383 Wrocław, Poland

Received December 28, 1995[⊗]

The hydrolysis of the monomeric five-coordinate (2-BzO-TPP)$Mn^{III}Cl$ complex has been investigated.[1] Evidence for the formation of the cyclic trimeric complex $[(2\text{-O}-\text{TPP})Mn^{III}]_3$ is presented. The ^1H NMR spectroscopic evidence indicates that the trimeric manganese(III) complex has a head-to-tail cyclic trimeric structure with the pyrrolic alkoxide groups forming bridges from one macrocycle to the manganese(III) ion in the adjacent macrocycle $\overline{\text{PMn}-\text{O}-\text{PMn}-\text{O}-\text{PMn}-\text{O}}$. The three manganese(III) porphyrin subunits are not equivalent. The characteristic upfield shift of the 3-H pyrrole resonance (−111.5 ppm at 291 K) was determined and considered as the diagnostic feature for the high-spin d^4 manganese(III)−pyrrole alkoxide coordination. The strong upfield shift of the 3-H resonance has been accounted for by the donation of the electron density from the filled orbital of the 2-O atom on the half-occupied d_{z^2} orbital of the external manganese(III) ion. The other pyrrole resonances produce the complex multiplet at the typical −5 to −40 ppm region. The ^1H NMR spectra of the series of monomeric 2-substituted manganese(III) 5,10,15,20-tetraphenylporphyrin complexes (2-X-TPP)$Mn^{III}Cl$ have been obtained and analyzed. The pattern of the assigned seven pyrrole resonances reflects the asymmetry imposed by 2-substitution and has been used as a ^1H NMR spectroscopic probe to map the spin density distribution. The electronic effect is strongly localized at the β-substituted pyrrole. The upfield shift of the 3-H resonance increases in the order (2-NO_2-TPP)$Mn^{III}Cl$ < (2-BzO-TPP)$Mn^{III}Cl$ < (2-OCH_3-TPP)$Mn^{III}Cl$ < (2-OH-TPP)$Mn^{III}Cl$ < (2-NH_2-TPP)$Mn^{III}Cl$ < $[(2\text{-O-TPP})Mn^{III}(OH)]^-$ following the increasing electron-donating properties of the β-substituent.

Introduction

The ability of porphyrin ligands to stabilize a large variety of manganese oxidation states has led to many interesting properties and potential application of these complexes. One of the areas of fundamental interest involves their use as catalysts in the oxidation of organic substrates.[2] These compounds have been investigated as models for peroxidase,[3] ligninase,[4] and transmembrane electron-transfer[5] or water-splitting reagents.[6] In addition, these complexes have been applied in NMR image enhancement,[7] as nonlinear optical materials,[8] and as DNA cleavage agents.[9] The cationic manganese porphyrin derivatives exhibit anti-HIV activity at micromolar concentrations.[10]

Despite considerable interest in monomeric manganese(III) porphyrins (i.e., in the oxidation state found under typical conditions), there has been little attention given to the formation of dimeric or polymeric derivatives. Insertion of the manganese(III) in 5-(2-hydroxyphenyl)-10,15,20-tritolylporphyrin ($TTOPH_2$) or in 5-hydroxyoctaethylporphyrin (oxophlorin, $OEPOH_2$) resulted in the formation of the manganese(III) doubly oxo bridged head-to-tail dimers $[(TTOP)Mn^{III}]_2$ and $[(OEPO)Mn^{III}]_2$, respectively.[11,12] By means of ^1H NMR, Goff et al. characterized the manganese(III) dimer $[(TTOP)Mn^{III}]_2$ and detected the diphenoxo-bridged heteronuclear complex [(TTOP)-Fe^{III}(TTOP)Mn^{III}].[11] The isolation and characterization of the dimanganese(IV) μ-oxo-bridged porphyrin complexes [(X)-$Mn^{IV}(TPP)]_2O$, $[(X)Mn^{IV}(TPP)]O[Mn^{III}(TPP)(X)]^+$ (X = N_3^-, OCN^-), and $[(X)Mn^{IV}(TPP)(OIPh)]_2O$ (X = Cl^-, Br^-) and μ-hydroxo-bridged dimanganese(III) bis-octaethylporphyrin complex were also reported.[13,14] Dimanganese(III) complexes of dimers of porphyrins linked by aromatic spacers provide

[⊗] Abstract published in *Advance ACS Abstracts,* July 1, 1996.

(1) Abbreviations used: P, porphyrin dianion; TPP, 5,10,15,20-tetraphenylporphyrin dianion; OEP, octaethylporphyrin dianion; TTOP, 5-(2-hydroxyphenyl)-10,15,20-tritolylporphyrin trianion; OEPO, 5-hydroxyoctaethylporphyrin (oxophlorin) trianion; 2-OH-TPP, dianion of 2-hydroxy-5,10,15,20-tetraphenylporphyrin; 2-O-TPP, trianion of 2-hydroxy-5,10,15,20-tetraphenylporphyrin; 2-OH-TPP-d_6, dianion of 2-hydroxy-5,10,15,20-tetraphenylporphyrin deuterated at unsubstituted pyrrole rings; 2-O-TPP-d_6, corresponding deuterated trianion; 2-BzO-TPP, dianion of 2-(benzoyloxy)-5,10,15,20-tetraphenylporphyrin; TMP, dianion of 5,10,15,20-tetramesitylporphyrin.

(2) (a) Meunier, B. *Chem. Rev.* **1992**, *92*, 1411. (b) Pratviel, G.; Bernadou, J.; Meunier, B. *Angew. Chem., Int. Ed. Engl.* **1995**, *34*, 746.
(3) Nick, R. J.; Ray, G. B.; Fish, K. M.; Spiro, T. G.; Groves, J. T. *J. Am. Chem. Soc.* **1991**, *113*, 1838.
(4) Labat, G.; Meunier, B. *J. Org. Chem.* **1989**, *54*, 5008.
(5) Nango, M.; Mizusawa, A.; Miyake, T.; Yoshinaga, J. *J. Am. Chem. Soc.* **1990**, *112*, 1640.
(6) Naruta, Y.; Sasayama, M.; Sasaki, T. *Angew. Chem., Int. Ed. Engl.* **1994**, *33*, 1839.
(7) Kellar, K. E.; Foster, N. *Inorg. Chem.* **1992**, *31*, 1353.
(8) Suslick, K. S., Chen, C.-T.; Meredith, G. R.; Cheng, L.-T. *J. Am. Chem. Soc.* **1992**, *114*, 6928.
(9) Pratviel, G.; Duarte, V.; Bernadou, J.; Meunier, B. *J. Am. Chem. Soc.* **1993**, *115*, 7939.
(10) Ding, L.; Balzarini, J.; Schols, D.; Meunier, B.; De Clercq, E. *Biochem. Pharmacol.* **1992**, *44*, 1675.
(11) Godziela, G. M.; Tilotta, D.; Goff, H. M. *Inorg. Chem.* **1986**, *25*, 2142.
(12) Balch, A. L.; Noll, B. C.; Reid, S. M.; Zovinka, E. P. *Inorg. Chem.* **1993**, *32*, 2610.
(13) (a) Schardt, B. C.; Hollander, F. J.; Hill, C. L. *J. Am. Chem. Soc.* **1982**, *104*, 3964. (b) Smegal, J. A.; Schardt, B. C.; Hill, C. L. *J. Am. Chem. Soc.* **1983**, *105*, 3510.
(14) Cheng, B.; Cukiernik, F.; Fries, P. H.; Marchon, J.-C.; Scheidt, W. R. *Inorg. Chem.* **1995**, *34*, 4627.

S0020-1669(95)01663-6 CCC: $12.00

alternative structural examples of dimeric manganese porphyrins.[15,16] A single example of manganese porphyrin incorporated into a polymeric backbone is exemplified by [PMn^{III}(imidazolate)]$_n$.[17] Finally, the manganese(III) complex with the octaethylbilindione tetrapyrrole unit (OEB; the product of the porphyrin degradation, which contains two keto groups at the opposite ends) [(OEB)Mn^{III}]$_2$ is dimeric with two helical (OEB)-Mn^{III} moieties of like chirality, joined together by O−Mn bonds to give a dimeric C_2 symmetry.[18]

Recently we have synthesized and characterized the unprecedented cyclic iron(III) porphyrin and gallium(III) porphyrin trimers (i.e., [(2-O-TPP)Fe^{III}]$_3$ and [(2-O-TPP)Ga^{III}]$_3$).[19,20] The trimers were generated through oligomerization of iron(III) 2-hydroxy-5,10,15,20-tetraphenylporphyrin and gallium(III) 2-hydroxy-5,10,15,20-tetraphenylporphyrin, respectively. The 2-hydroxy-5,10,15,20-tetraphenylporphyrin molecule presents properties of hybrid bifunctional ligands, since it contains two centers of coordination, four internal pyrrolic nitrogens, and an external 2-OH group. The trivalent metal coordinated in the porphyrin macrocycle seems to be a prerequisite of the trimer formation. Only the monomeric species were reported for the series of divalent metal ions.[21]

Here, we sought to extend the group of the cyclic metalloporphyrin trimers by the analogous manganese(III) species. To determine the trimeric structure, we have taken full advantage of our previous investigations of paramagnetic iron(III) and diamagnetic gallium(III) complexes in which we established the ^{1}H NMR spectroscopic evidence for the cyclic trimer formation. In this article, we are concerned with using ^{1}H NMR spectroscopy as a structural probe to identify paramagnetic β-hydroxy-(methoxy)-substituted manganese(III) porphyrins since the pyrrole protons of paramagnetic manganese porphyrins have been shown to be particularly diagnostic of changes in spin, oxidation, and ligation states.[13,22−36]

Results and Discussion

Characterization of (2-BzO-TPP)Mn^{III}Cl. In order to produce manganese(III) 2-hydroxytetraphenylporphyrin complexes, the β-(benzoyloxy) derivative (2-BzO-TPP)Mn^{III}Cl was prepared by a route that involves benzoyloxation of tetraphenylporphyrin, followed by the chromatographic separation of the product and subsequent manganese insertion into 2-BzO-TPPH$_2$.[19,20,37] The electronic spectrum of (2-BzO-TPP)Mn^{III}Cl presented in Figure 1 is typical of manganese(III) tetraphenylporphyrins.[38]

The β-substitution markedly lowers the symmetry of the manganese(III) porphyrin from the effective C_{4v} symmetry of the analogous (TPP)Mn^{III}Cl. This is poorly reflected in the ^{1}H NMR spectrum of (2-BzO-TPP)Mn^{III}Cl (Figure 2, Table 1). The ligand asymmetry is only reflected by the asymmetric shape of the pyrrole multiplet. The position of the multiplet center is typical for manganese(III) tetraphenylporphyrins. The phenyl protons produce a rather uncharacteristic set of strongly overlapped lines in the 7−10 ppm region. A more distinct spread of the pyrrole resonances has been found for other β-substituted manganesese(III) tetraphenylporphyrins as presented in Figure 2 and discussed later.

Synthesis and Characterization of [(2-O-TPP)Mn^{III}]$_3$. Ethanolysis of (2-BzO-TPP)Mn^{III}Cl resulted in the formation of a trimeric molecule (eq 1).

$$3(\text{2-BzO-TPP})\text{Mn}^{III}\text{Cl} + 6\text{NaOH} \xrightarrow{\text{EtOH, then } H_2O} [(\text{2-O-TPP})\text{Mn}^{III}]_3 + 3\text{NaOBz} + 3\text{NaCl} + 3\text{H}_2\text{O} \quad (1)$$

[(2-O-TPP)Mn^{III}]$_3$ has been characterized by a range of spectroscopic methods. The electronic spectrum of [(2-O-TPP)-Mn^{III}]$_3$ is presented in Figure 1 together with the spectra of (2-BzO-TPP)Mn^{III}Cl and [(2-O-TPP)Mn^{III}(OH)]$^-$ (vide infra). The compounds (2-OH-TPP)Mn^{III}Cl, (2-OCH$_3$-TPP)Mn^{III}Cl, and (2-BzO-TPP)Mn^{III}Cl (discussed previously) demonstrate characteristics of d-type hyperporphyrin spectra with pronounced splitting of the Soret band.[38] The electronic spectrum of [(2-O-TPP)Mn^{III}]$_3$ differs considerably from its monomeric precursors and from any high-spin five-coordinate manganese(III) tetraphenylporphyrin with an oxygen donor at the axial position.[26−28,33,39] The splitting of the Soret band is absent, and all bands are broadened as compared to those of (2-BzO-TPP)-Mn^{III}Cl. The differences may be induced by the 2-O axial ligand coordination and/or by the porphyrin−porphyrin π− interaction caused by the proximity of the porphyrin rings in the close-packed trimeric structure.[40] The magnetic susceptibility of [(2-O-TPP)Mn^{III}]$_3$ is somewhat lower than typical of a manganese(III) porphyrin. The magnetic moment as measured by the Evans technique[41] in chloroform solution at 293 K equals 4.6 μ_B per manganese atom. The typical value of $\mu = 4.8$ μ_B has been determined for (2-OH-TPP)Mn^{III}Cl generated from the original sample of [(2-O-TPP)Mn^{III}]$_3$ by splitting with gaseous HCl directly in the NMR tube. This value is similar to that of (TPP)Mn^{III}Cl (4.9 μ_B).[42] The minor lowering of the magnetic

(15) Naruta, Y.; Sasayama, M. *J. Chem. Soc., Chem. Commun.* **1994**, 2667.
(16) (a) Landrum, J. T.; Grimmett, D.; Haller, K. J.; Scheidt, W. R.; Reed, C. A. *J. Am. Chem. Soc.* **1981**, *103*, 2640. (b) Collman, J. P.; Bencosme, C. S.; Durand, R. R., Jr.; Kreh, R. P.; Anson, F. C. *J. Am. Chem. Soc.* **1983**, *105*, 2699.
(17) Landrum, J. T.; Hatano, K.; Scheidt, W. R.; Reed, C. A.; *J. Am. Chem. Soc.* **1980**, *102*, 6729.
(18) Balch, A. L.; Mazzanti, M.; Noll, B. C.; Olmstead, M. M. *J. Am. Chem. Soc.* **1994**, *116*, 9114.
(19) Wojaczyński, J.; Latos-Grażyński, L. *Inorg. Chem.* **1995**, *34*, 1044.
(20) Wojaczyński, J.; Latos-Grażyński, L. *Inorg. Chem.* **1995**, *34*, 1054.
(21) (a) Crossley, M. J.; King, L. G.; Pyke, S. M. *Tetrahedron* **1987**, *43*, 4569. (b) Crossley, M. J.; Harding, M. M.; Sternhell, S. *J. Am. Chem. Soc.* **1986**, *108*, 3608. (c) Crossley, M. J.; Field, L. D.; Harding, M. M.; Sternhell, S. *J. Am. Chem. Soc.* **1987**, *109*, 2335. (d) Crossley, M. J.; Harding, M. M.; Sternhell, S. *J. Org. Chem.* **1988**, *53*, 1132. (e) Crossley, M. J.; Burn, P. L.; Langford, S. J.; Pyke, S. M.; Stark, A. G. *J. Chem. Soc., Chem. Commun.* **1991**, 1567.
(22) La Mar, G. N.; Walker (Jensen), F. A. In *The Porphyrins*; Dolphin, D., Ed.; Academic Press: New York, 1978; Vol. 4, p 61.
(23) Bertini, I.; Luchinat, C. *NMR of Paramagnetic Molecules in Biological Systems*; The Benjamin/Cummings Publishing Co.: Reading, MA, 1986.
(24) (a) La Mar, G. N.; Walker, F. A. *J. Am. Chem. Soc.* **1973**, *95*, 6950. (b) La Mar, G. N.; Walker, F. A. *J. Am. Chem. Soc.* **1975**, *97*, 5103.
(25) Goff, H. M.; Hansen, A. P. *Inorg. Chem.* **1984**, *23*, 321.
(26) (a) Hill, C. L.; Williamson, M. M. *Inorg. Chem.* **1985**, *24*, 2836. (b) Hill, C. L.; Williamson, M. M. *Inorg. Chem.* **1985**, *24*, 3024.
(27) Arasasingham, R. D.; Bruice, T. C. *Inorg. Chem.* **1990**, *29*, 1422.
(28) Turner, P.; Gunter, M. J. *Inorg. Chem.* **1994**, *33*, 1406.
(29) Hansen, A. P.; Goff, H. M. *Inorg. Chem.* **1984**, *23*, 4519.
(30) VanAtta, R. B.; Strouse, C. E.; Hanson, L. K.; Valentine, J. S. *J. Am. Chem. Soc.* **1987**, *109*, 1425.
(31) Hill, C. L.; Hollander, F. J. *J. Am. Chem. Soc.* **1982**, *104*, 7318.
(32) Groves, J. T.; Stern, M. K. *J. Am. Chem. Soc.* **1988**, *110*, 8628.
(33) Groves, J. T.; Watanabe, Y.; McMurry, T. J. *J. Am. Chem. Soc.* **1983**, *105*, 4489.
(34) Shirazi, A.; Goff, H. M. *J. Am. Chem. Soc.* **1982**, *104*, 6318.
(35) Valentine, J. S.; Quinn, A. E. *Inorg. Chem.* **1976**, *15*, 1997.
(36) Rodgers, K. R.; Goff, H. M. *J. Am. Chem. Soc.* **1988**, *110*, 7049.
(37) Callot, H. *Bull. Soc. Chim. Fr.* **1974**, 1492.
(38) Gouterman, M. In *The Porphyrins*; Dolphin, D., Ed.; Academic Press: New York, 1978; Vol. 3, Part A, Chapter 1.
(39) Williamson, M. M.; Hill, C. L. *Inorg. Chem.* **1986**, *25*, 4668.
(40) (a) Osuka, A.; Maruyama, K. *J. Am. Chem. Soc.* **1988**, *110*, 4454. (b) Chang, C. K. *Adv. Chem. Ser.* **1979**, *173*, 162. (c) Hunter, C. A.; Sanders, J. K. M. *J. Am. Chem. Soc.* **1990**, *112*, 5525.
(41) (a) Evans, D. F.; James, T. A. *J. Chem. Soc., Dalton Trans.* **1979**, 723. (b) Sur, S. K. *J. Magn. Reson.* **1989**, *82*, 169.
(42) Behere, D. V.; Mitra, S. *Inorg. Chem.* **1980**, *19*, 992.

Table 1. NMR Data for Manganese Porphyrins

compound	spin state	solvent	nucleus	δ pyrrole (ppm)	T (K)	ref
$TPPMn^{II}$	$^5/_2$	DMSO	^2H	34	298	34
$TPPMn^{III}Cl$	2	CD_2Cl_2	^1H	−22	298	24b
$[TPPMn^{III}O_2]^-$	2	DMSO	^2H	32	298	30
$[TPPMn^{III}(Im)_2]^-$	1	DMSO-d_6	^1H	−18	299	29
$[TPPMn^{III}(CN)_2]^-$	1	DMSO-d_6	^1H	−15	299	29
$[(^{\bullet}TMP)Mn^{III}Cl]SbCl_6$	2, $^1/_2$	CH_2Cl_2	^2H	−40	298	27
$(TMP)Mn^{IV}(OCH_3)_2$	$^3/_2$	toluene	^2H	−16	298	27
$TMPMn^{IV}O$	$^3/_2$	CH_2Cl_2	^2H	−32	233	32
$[TPPMn^{IV}(OCN)]_2O$	*a*	$CDCl_3$	^1H	7	283	14
$TMPMn^{V}N$	0	$CDCl_3$	^1H	9	293	31
$[(2\text{-}O\text{-}TPP)Mn^{III}]_3$	2	$CDCl_3$	^1H	−111.5[b] (3H), −35.9 (2H), −31.9, −30.2, −26.4, −23.7 (2H), −22.2, −19.1 (3H), −14.4 (2H), −11.6 (2H), −10.1 (3H)	291	*c*
$(2\text{-}BzO\text{-}TPP)Mn^{III}Cl$	2	$CDCl_3$	^1H	−23 (7H)	295	*c*
$(2\text{-}OH\text{-}TPP)Mn^{III}Cl$[d]	2	$CDCl_3$	^1H	−43,[b] −30, −24 (3H), −18 (2H)	295	*c*
$(2\text{-}OCH_3\text{-}TPP)Mn^{III}Cl$	2	$CDCl_3$	^1H	−40,[b] −30, −26, −23 (2H), −19 (2H)	293	*c*
$[(2\text{-}O\text{-}TPP)Mn^{III}(OH)]^-$	2	$CDCl_3$	^1H	−74,[b] −32, −28, −17 (2H), −2[e]	293	*c*
$(2\text{-}NO_2\text{-}TPP)Mn^{III}Cl$	2	$CDCl_3$	^1H	−24 (4H), −17 (2H), −13[b]	295	*c*
$(2\text{-}NH_2\text{-}TPP)Mn^{III}Cl$[f]	2	$CDCl_3$	^1H	−56,[b] −34, −28, −23 (2H), −14 (2H)	295	*c*

[a] Antiferromagnetically coupled. [b] 3-H pyrrole resonance. [c] This work; *meso* phenyl resonances in 10−7 ppm region. [d] OH resonance at −4.4 ppm. [e] Not all pyrrole resonances visible. [f] NH_2 resonance at −9.2 ppm.

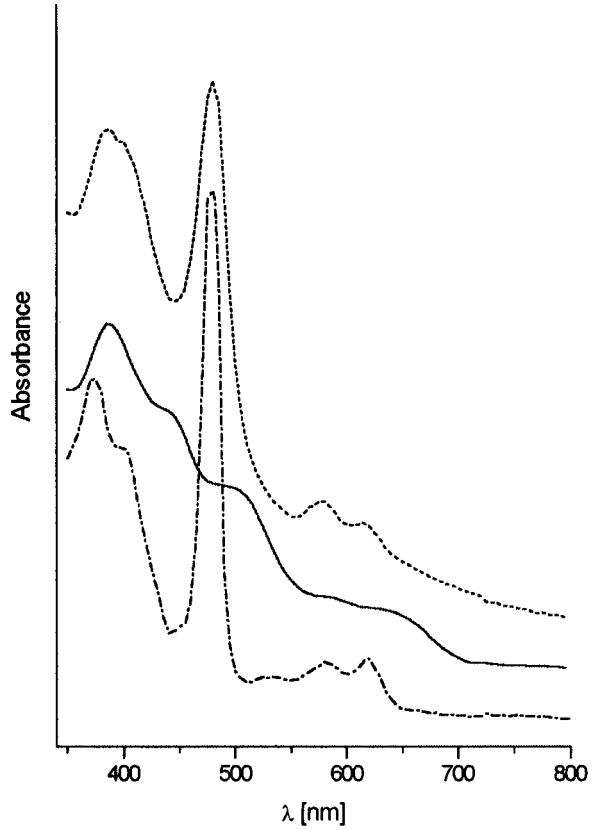

Figure 1. UV−vis spectra of $(2\text{-}BzO\text{-}TPP)Mn^{III}Cl$ (dot-dashed line), $[(2\text{-}O\text{-}TPP)Mn^{III}]_3$ (solid line), and $[(2\text{-}O\text{-}TPP)Fe^{III}(OH)]^-$ (dashed line) in dichloromethane.

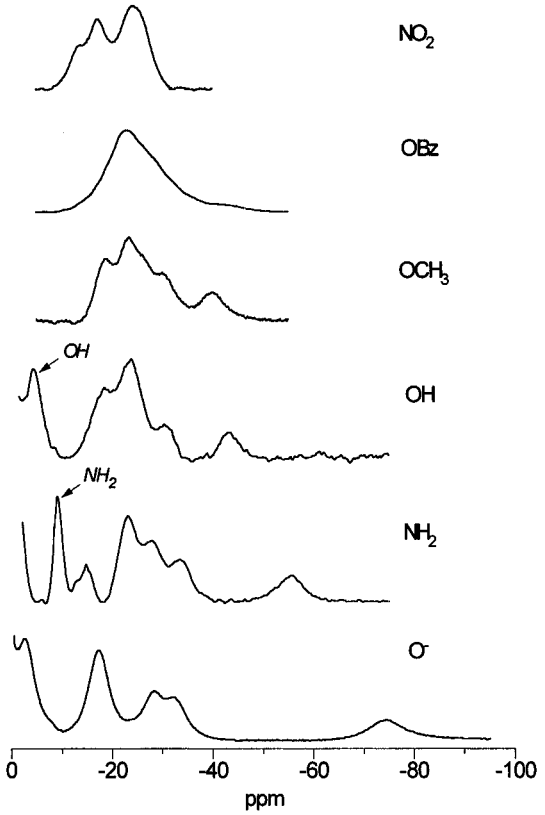

Figure 2. Pyrrole region of the 300 MHz ^1H NMR spectra of mono-β-substituted manganese porphyrins $(2\text{-}X\text{-}TPP)Mn^{III}Y$ in chloroform-*d* solutions at 293−295 K. The respective X substituents shown on each trace, and Y = Cl for all complexes, except Y = OH for $[(2\text{-}O\text{-}TPP)Mn^{III}(OH)]^-$. The OH and NH_2 resonances are labeled separately.

moment for the trimer with respect to the monomeric manganese(III) porphyrins is due to the weak antiferromagnetic coupling.

The liquid matrix secondary ion mass spectrum of $[(2\text{-}O\text{-}TPP)Mn^{III}]_3$ primarily shows peaks due to the trimer and its stepwise deoligmerization products $[(2\text{-}O\text{-}TPP)Mn^{III}]_2$ at $(m + 1)/z = 1365$ (13.3%) and $[(2\text{-}O\text{-}TPP)Mn^{III}]$ at $(m + 1)/z = 683$ (100%). The reproducible peak of the parent species $[(2\text{-}O\text{-}TPP)Mn^{III}]_3$ at $(m + 1)/z = 2047$ (0.6%) was seen as well. Solely on the basis of the mass spectrum, we cannot rule out structures higher than trimeric oligomers, since larger ions might not survive in the gas phase. In our experiment, the most intense peak corresponds to the monomeric unit. However, only the trimeric formula is consistent with the ^1H NMR data.

^1H NMR Spectroscopic Studies of $[(2\text{-}O\text{-}TPP)Mn^{III}]_3$. The ^1H NMR spectrum of $[(2\text{-}O\text{-}TPP)Mn^{III}]_3$ is shown in Figure 3. The resonance assignments, shown in Table 1, have been made on the basis of relative intensities, line width analysis, and site specific deuteration. The ^1H NMR parameters of monomeric $(2\text{-}OH\text{-}TPP)Mn^{III}Cl$, $(2\text{-}OCH_3\text{-}TPP)Mn^{III}Cl$, $(2\text{-}NH_2\text{-}TPP)Mn^{III}Cl$, $(2\text{-}NO_2{-}TPP)Mn^{III}Cl$, $(2\text{-}BzO\text{-}TPP)Mn^{III}Cl$, and $[(2\text{-}O\text{-}TPP)Mn^{III}(OH)]^-$ are also gathered in Table 1, together with representative examples of manganese tetrarylporphyrins in

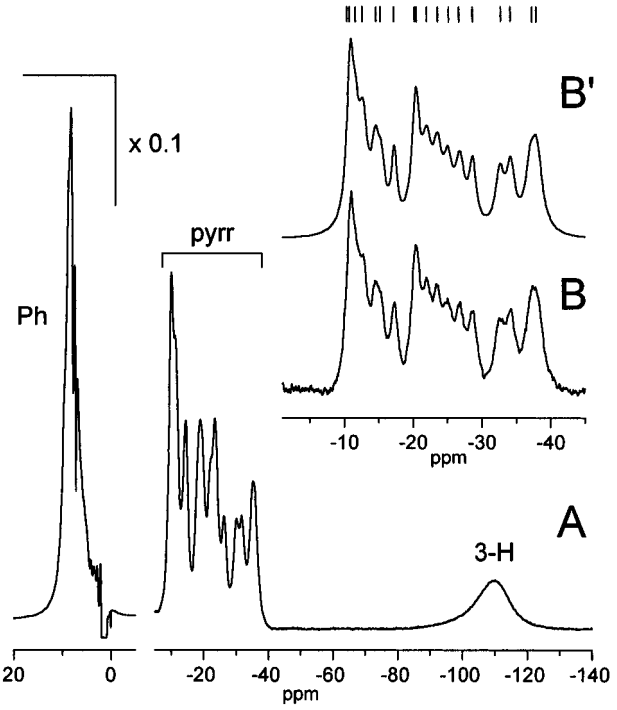

Figure 3. 300 MHz ^{1}H NMR spectra of [(2-O-TPP)Mn^{III}]$_3$ in chloroform-*d* solution. Trace A shows the entire spectrum obtained using the inversion−recovery technique at 291 K. Intensity of the phenyl region (20 to −5 ppm) is reduced 10 times for better presentation. Trace B presents the pyrrole region of the spectrum collected at 283 K to achieve the best resolution of resonances. Trace B′ demonstrates the convolution of 18 resonances of similar line width and intensity of one proton each used to reproduce the spectrum shown in trace B. Line positions are shown by tick marks. Resonance assignments: pyrr, pyrrole protons; Ph, *meso* phenyl protons; 3-H, the resonance of 3-H proton.

accessible electronic/spin/oxidation/ligation states. In order to identify phenyl and pyrrole resonances, the ^{1}H NMR spectrum of [(2-O-TPP-d_6)Mn^{III}]$_3$ (deuterated at the 7, 8, 12, 13, 17, and 18 pyrrolic positions) have been obtained, and the diminished intensity of pyrrole resonances in the −5 to −40 ppm region has been found. The proton resonances can be easily separated into three groups (Figure 3). The most characteristic feature, a strong, very broad upfield-shifted peak at −111.5 ppm (291 K) with intensity of three protons, corresponds to the 3-H pyrrole positions. The remaining pyrrole protons produce resonances in the −5 to −40 ppm region. Thirteen clearly resolved resonances (at 283 K), some of them partially overlapped, are present. We have applied the deconvolution procedure to this part of the spectrum in order to demonstrate that 18 resonances of similar line widths (350−550 Hz) and intensities of one proton each are required to reproduce the experimental spectrum (Figure 3, trace B′). Using the same procedure, we have determined that the intensity of the resonance at −111.5 ppm corresponds to three pyrrole protons. The phenyl resonances present a complex, barely resolved pattern which is spread over the 7−10 ppm range (Figure 3, trace A). On the basis of the complex symmetry, the 60 different phenyl resonances should be potentially traced in this region. They are located in the region usually expected for manganese(III) tetraphenylporphyrins. The average shift of the pyrrole resonances located in the −5 to −40 ppm region (291 K) equals −20.5 ppm. This is close to the value characteristic for monomeric manganese(III) porphyrin complexes (see Table 1).

The spectroscopic evidence indicates that the manganese(III) complex has a head-to-tail trimeric structure, with the pyrrolic alkoxide groups forming the bridges from one macrocycle to the metal ion of the adjacent macrocycle. A schematic view of the proposed porphyrin skeleton analogous to [(2-O-TPP)-Fe^{III}]$_3$ and [(2-O-TPP)Ga^{III}]$_3$ is presented in Figure 4.[19,20] The manganese(III) ions are located at corners of an equilateral triangle at a distance of ca. 7 Å.

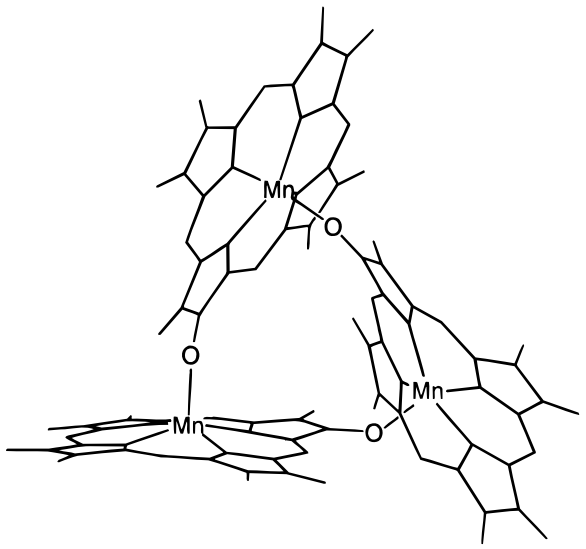

Figure 4. Schematic view of the porphyrin skeleton of [(2-O-TPP)-Mn^{III}]$_3$. Phenyl rings are omitted for clarity.

Such an oligomeric structure accounts for the mass of the largest ion in the mass spectrometry. The ^{1}H NMR spectrum clearly points toward three distinct manganese(III) porphyrin units in the complex, indicated by the upfield pyrrole resonance accompanied by the multiplet of remaining pyrrole resonances. The multiplet is composed of three sets of six resonances, each corresponding to a different unit. The unprecedented upfield hyperfine shift of the 3-H resonances can be explained only by the direct coordination of the β-oxygen to the external manganese(III) ion required by oligomerization. Finally, the alternative linear trimeric structure would require an OH resonance in the 0 to −10 ppm region (not observed for [(2-O-TPP)Mn^{III}]$_3$) and an intensity of two protons for the 3-H pyrrole resonances in the upfield part of spectrum, instead of the intensity of three protons determined experimentally.

Formally, manganese(III) 2-hydroxytetraphenylporphyrin (2-OH-TPP)Mn^{III}X can be used as a building block in the oligomerization discussed in detail for [(2-O-TPP)Fe^{III}]$_3$.[19] This five-coordinate complex exists as two optical antipodes (*R*, *S*). The five-coordinate insertion product of manganese(III) into 2-OH-TPPH$_2$ (i.e., (2-OH-TPP)Mn^{III}X) has an optical asymmetry associated with the direction of the axial ligand approach to the manganese(III) ion. The random selection of the *R* and *S* enantiomers from the racemic mixture of (2-OH-TPP)Mn^{III}X to form trimers should produce the following stereoisomers: *RRR*, *RRS*, *RSS*, and *SSS*. Only the *RRS* (*SSR*) structure is consistent with the examined ^{1}H NMR spectrum observed previously for similar cyclic trimers of gallium(III) and iron(III).[19,20]

Cleavage of [(2-O-TPP)Mn^{III}]$_3$. Addition of HCl in excess to [(2-O-TPP)Mn^{III}]$_3$ results in cleavage of the trimer according to eq 2. Figure 2 shows the corresponding ^{1}H NMR spectrum.

$$[(2\text{-O-TPP})\text{Mn}^{III}]_3 + 3\text{HCl} \rightarrow 3(2\text{-OH-TPP})\text{Mn}^{III}\text{Cl} \quad (2)$$

Its features are consistent with the formation of the (2-OH-TPP)-Mn^{III}Cl complex. The considerable simplification of the spectral pattern is observed. The upfield 3-H pyrrole resonances, the most characteristic for [(2-O-TPP)Mn^{III}]$_3$, disappeared, and four

new pyrrole resonances (the intensity ratio of 2:3:1:1) are found in the −5 to −55 ppm region. They correspond to seven pyrrole protons which are unequivalent due to the β-substitution. The pyrrole resonances of (2-OH-TPP)$Mn^{III}Cl$ have nearly equal line widths, and the differential broadening of the pyrrole resonances determined for the trimeric molecule is absent. The *meso* phenyl resonances are observed in the 7−10 ppm region as expected for manganese(III) tetraphenylporphyrin. A unique resonance at −4.4 ppm for (2-OH-TPP)$Mn^{III}Cl$ has been assigned to the β-hydroxyl proton. When chloroform-*d* saturated with deuterium oxide was added to a solution of (2-OH-TPP)$Mn^{III}Cl$, the 2-OH resonance disappeared. The resonance at −43 ppm for (2-OH-TPP)$Mn^{III}Cl$ has been assigned to the 3-H position of the β-substituted pyrrole by comparison of ^{1}H NMR spectra of (2-OH-TPP)$Mn^{III}Cl$ and (2-OH-TPP-d_6)$Mn^{III}Cl$ (not shown). The selective deuteration of all but the 3-H position has been determined for (2-OH-TPP-d_6)$Mn^{III}Cl$.

The addition of an excess of hydroxide ion in methanolic solution to a solution of $[(2\text{-O-TPP})Mn^{III}]_3$ in chloroform-*d* results in its conversion to the five-coordinate, monomeric complex:

$$[(2\text{-O-TPP})Mn^{III}]_3 + 3OH^- \rightarrow 3[(2\text{-O-TPP})Mn^{III}(OH)]^- \quad (3)$$

The effect of adding hydroxide anion is shown in Figure 2. Five observed upfield resonances were assigned to pyrrole protons. In particular, the 3-H resonance occurs at −74 ppm. The assignment of the 3-H resonance is given by the comparison of the $[(2\text{-O-TPP})Mn^{III}(OH)]^-$ and $[(2\text{-O-TPP-}d_6)Mn^{III}(OH)]^-$ spectra. The addition of water to the chloroform solution of $[(2\text{-O-TPP})Mn^{III}(OH)]^-$ results in the reconversion to the trimer.

Keto−Enol Tautomerism in (2-OH-TPP)$Mn^{III}Cl$. During the synthesis of the pyrrole-deuterated $[(2\text{-O-TPP})Mn^{III}]_3$, we have observed the increased lability of the 3-H proton. The usual procedure of the trimer synthesis has been modified by the replacement of (2-BzO-TPP)$Mn^{III}Cl$ with (2-BzO-TPP-d_7)$Mn^{III}Cl$ (80% deuteration at pyrrole positions as shown by ^{1}H NMR). The intensity of the upfield-shifted pyrrole resonances has been partially recovered in the ^{1}H NMR spectrum of $[(2\text{-O-TPP-}d_6)Mn^{III}]_3$ (not shown) contrary to the reduced intensity of the remaining pyrrole resonances. The acidic cleavage of $[(2\text{-O-TPP-}d_6)Mn^{III}]_3$, followed by ^{1}H NMR, produced the spectrum of (2-OH-TPP-d_6)$Mn^{III}Cl$ with the partially recovered intensity of the 3-H resonance. To account for the process of the deuterium−proton exchange, we have considered the keto−enol tautomerism, established by Crossley et al.[21] for zinc(II) and copper(II) complexes of 2-hydroxytetraphenylporphyrin and observed also in our investigation[19,20] on gallium(III) and iron(III) complexes. The keto−enol tautomerism allows the replacement of the predeuterated 3-D position by 3-H under the basic conditions of the trimerization.

Analysis of Paramagnetic Shifts in Terms of the Structure of $[(2\text{-O-TPP})Mn^{III}]_3$. In general, the isotropic shifts of manganese(III) tetrarylporphyrins were shown to be predominantly contact in origin, reflecting extensive porphyrin-to-metal π-bonding.[22−28] The isotropic shifts for the *meso* aryl resonances are very small, ruling out appreciable dipolar contribution at any other positions. The β-H pyrrole resonances demonstrate upfield contact shifts consistent with the $d_{x^2-y^2}$ orbital being unoccupied and the d_{xz} and d_{yz} orbitals being partially occupied. Such a spectral pattern can be accounted for by the $(d_{xy})^1(d_{xz})^1(d_{yz})^1(d_{z^2})^1$ ground state electronic configuration ($PMn^{III}X$, $S = 2$).[24−26] A recently suggested valence isomeric form, which corresponds formally to the manganese(II) cation radical porphyrin ($P^{\bullet}$)$Mn^{II}X$, (P, porphyrin; X, axial ligand) with two paramagnetic centers ($S = {}^3/_2$, $S = {}^1/_2$), may also be involved.[28] The electronic structure of ($P^{\bullet}$)$Mn^{II}X$ $(d_{xy})^2(d_{xz})^1(d_{yz})^1(d_{z^2})^1(a_2(\pi))^1(a_1(\pi))^2$ [$a_2(\pi)$ and $a_1(\pi)$ represent the HOMO orbitals of porphyrin dianion] accounts for the upfield shift of the β-H resonances and is consistent with the spin density distribution determined by ^{13}C NMR in the carbon skeleton of (TPP)$Mn^{III}X$.[28]

We have noticed that the manganese complexes investigated in this work belong to the large series of 2-substituted manganese(III) 5,10,15,20-tetraphenylporphyrin monomeric complexes of the general formula (2-X-TPP)$Mn^{III}Cl$. To get the proper perspective in the analysis of the paramagnetic shift, we have extended the group of investigated monomeric complexes in order to probe the influence of the β-substituent on the position of the analytically crucial 3-H resonance. The relevant spectra of the two complexes, containing the strongly electron-withdrawing and strongly electron-donating substituents (i.e., (2-NO_2-TPP)$Mn^{III}Cl$ and (2-NH_2-TPP)$Mn^{III}Cl$) have been also considered and are demonstrated in Figure 2 and in Table 1.

The ^{1}H NMR spectra of (2-X-TPP)$Mn^{III}Cl$ have been analyzed in the context of the low symmetry resulting from the β-substitution. There are seven distinct pyrrole positions instead of the single one for (TPP)$Mn^{III}X$. Consequently, there are seven expected upfield pyrrole resonances for (2-X-TPP)-$Mn^{III}Cl$. The six resonances are spread near the typical position for (TPP)$Mn^{III}Cl$. Since the line width of the pyrrole resonances is usually large (850−2000 Hz for the studied complexes), the convolution of resonances results in the multiplets where the number of resolved resonances depends on the extent of overlapping (Table 1). The upfield shift of the 3-H resonances varies considerably, increasing in the series (2-NO_2−TPP)-$Mn^{III}Cl$ (−13 ppm) < (2-BzO-TPP)$Mn^{III}Cl$ (∼ −23 ppm) < (2-OCH_3−TPP)$Mn^{III}Cl$ (−40 ppm) < (2-OH-TPP)$Mn^{III}Cl$ (−43 ppm) < (2-NH_2-TPP)$Mn^{III}Cl$ (−56 ppm) < $[(2\text{-O-TPP})Mn^{III}(OH)]^-$ (−74 ppm) (the 3-H shift at 293−296 K is given in parentheses). The very small isotropic shifts of the phenyl resonances point toward the negligible dipolar shift, allowing the conclusion that the spread of the pyrrole resonances is determined by the contact shift. Consequently, the ^{1}H NMR parameters map the spin density distribution in these 2-substituted porphyrins. The electronic effect is strongly localized at the β-substituted pyrrole. The position of the 3-H resonance correlates well with the electron-donating properties of the 2-substituents.

Recently, we have demonstrated similar dependencies of the 3-H contact shift with respect to the electron-withdrawing/donating properties of the 2-X substituents for high-spin iron(III) complexes (2-X-TPP)$Fe^{III}Cl$ and low-spin iron(III) complexes $[(2\text{-X-TPP})Fe^{III}(CN)_2]^-$.[43] The positions of 3-H resonances change on going to more electron-donating substituents in the following ranges: −1.5 to −44.0 ppm for low-spin complexes; 104.0 to 33.4 ppm for high-spin complexes.[43]

Therefore, one can conclude that three different electronic ground states (i.e., d^5 low-spin $(d_{xy})^2(d_{xz}d_{yz})^3$, d^4 high-spin $(d_{xy})^1(d_{xz})^1(d_{yz})^1(d_{z^2})^1$, d^5 high-spin $(d_{xy})^1(d_{xz})^1(d_{yz})^1(d_{z^2})^1(d_{x^2-y^2})^1$) are applying a similar π spin density mechanism, which accounts for the upfield relocation of the 3-H resonances. Obviously the β-substitutions have affected the patterns of the porphyrin molecular orbitals involved in the spin density transfer identically for each of these metal ion electronic structures.

The ^{1}H NMR spectra of $[(2\text{-O-TPP})Mn^{III}]_3$ show a number of remarkable features that must arise from its unusual molecular

(43) Wojaczyński, J.; Latos-Grażyński, L.; Hrycyk, W.; Pacholska, E.; Rachlewicz, K.; Szterenberg, L. Submitted.

structure. They can be understood in the context of the presence of three manganese(III) ions in the molecule. The β-hydroxyporphyrin of each monomeric unit is coordinated simultaneously to the internal manganese(III) through four nitrogens and to the external one by an oxygen. The characteristic features of the internal manganese(III) influence are exemplified by ^{1}H NMR spectra of (2-OH-TPP)Mn^{III}Cl and (2-OCH_3-TPP)Mn^{III}Cl discussed above. However, the presence of the second source of the spin density (i.e., the external manganese(III)) increases the upfield hyperfine shifts for the 3-H (*R*,*R*,*S*) protons. Assuming simple additivity of contact contributions by two independent routes, we have estimated that such a shift requires two upfield components of ca. −50 ppm (internal), found for (2-OH-TPP)-Mn^{III}Cl, and ca. −70 ppm (external).

The upfield contribution to the 3-H shift results mainly from the σ-donation of the electron density of the 2-O donor on the half-occupied d_{z^2} orbital of the manganese(III) ion. The anticipated positive spin density on the σ-orbital of the oxygen will be directly transferred into the π-system of the pyrrole ring without any manganese(III)−oxygen π-bonding. The ligand σ- and π-orbitals are not orthogonal, and $\sigma-\pi$ overlap within the ligand permits the direct spin density transfer.[19,44,45]

Considering the idealized geometry of coordination or the 2-hydroxypyrrole and phenoxide fragments, we suggest a similar delocalization mechanism to rationalize the upfield contact shifts of the protons located similarly with respect to the external manganese(III) ion.

The magnitudes of the hyperfine shifts of the phenoxide ortho protons in manganese(III) porphyrin complexes (−90 to −150 ppm)[11] are in the same direction as those evaluated for the external contact contribution of 3-H protons. The line width of the 3-H pyrrole resonances correlates with their specific locations within the trimeric structure. The dipolar contribution to line width broadening is presumed to be proportional to r^{-6}, where r is the distance from the paramagnetic manganese(III) center to the proton in question when the ligand-centered dipolar relaxation is insignificant.[22,23] The contribution from the internal manganese(III) ion via dipolar and scalar mechanisms has been approximated by the line widths of downfield pyrrole resonances which vary in the narrow range of 350−550 Hz. These lines are considerably more narrow than the pyrrole signals of monomeric 2-substituted manganese(III) porphyrins. The resonance assigned to 3-H protons exhibits a markedly larger line width (ca. 3000 Hz). Assuming the narrowest limit for three 3-H components, their line widths have been estimated to be one-third of the composed resonance (i.e., 1000 Hz), which is definitely much larger than that for other pyrrole resonances. The most likely additional contribution to the line width derives mainly from the dominant dipolar mechanism of the closely located external manganese(III) ion. Therefore, the pattern of pyrrole line width is qualitatively in agreement with the proposed molecular structure.

Conclusions

In our previous investigations of paramagnetic iron(III) and diamagnetic gallium(III) complexes, we have established "finger print" type diagnostic ^{1}H NMR spectroscopic evidence for the cyclic trimer formation in the self-assembly process of monomeric iron(III) 2-hydroxy-5,10,15,20-tetraphenylporphyrin or gallium(III) 2-hydroxy-5,10,15,20-tetraphenylporphyrin.[19,20] In the case of diamagnetic gallium porphyrin, there are three upfield-shifted pyrrole resonances at 1.82, 2.18, and 2.82 ppm (243 K). The paramagnetic iron porphyrin presents three unusually upfield-shifted 3-H pyrrole resonances at −89.8, −94.7, and −99.3 ppm at 293 K. In our opinion, the ^{1}H NMR spectral characteristics of the diamagnetic cyclic trimer is transferable to other diamagnetic metal ions.[46] On the other hand, paramagnetic cyclic trimers would require independent investigations to establish a relevant ^{1}H NMR spectral pattern dependent on the ground electronic state of the metal ion.

In this paper we have determined the formation of a paramagnetic manganese porphyrin cyclic trimer. Its characteristic large 3-H pyrrole upfield hyperfine shift (−111.5 ppm) clearly provides pyrrole resonances in the ^{1}H NMR window which are unique for cyclic manganese(III) porphyrin trimers. One can suggest that 2-hydroxy(oxo)-substituted manganese porphyrins might be involved in the degradation of manganese porphyrin catalysts in the presence of oxidizing substrates. The spectroscopic results of this investigation should be relevant to their identification.

Experimental Section

Solvents and Reagents. All solvents were purified by standard procedures. Tetraphenylporphyrin ($TPPH_2$) and $TPPH_2$-d_8 were prepared using reported methods.[47,48] Chloroform-*d* ($CDCl_3$, Glaser AG) was dried before use by passing through activated basic alumina.

Preparation of Compounds 2-BzO-$TPPH_2$, 2-OCH_3-$TPPH_2$, 2-NH_2-$TPPH_2$, and 2-NO_2-$TPPH_2$. These porphyrins were prepared by a standard procedure starting from $TPPH_2$.[19,20,21,37] The respective deuterated derivatives were obtained from the deuterated precursors.[19,20,43]

(2-BzO-TPP)Mn^{III}Cl. A solution of 1 g (5 mmol) of manganese(II) chloride tetrahydrate in 50 mL of ethanol was added to a solution of 73 mg (0.1 mmol) of 2-(benzoyloxy)tetraphenylporphyrin in 50 mL of chloroform. The solution was heated under reflux for 0.5 h. It was cooled, washed three times with water, and dried over anhydrous magnesium sulfate. After filtration, the solvent was removed on the rotary evaporator. The chloroform solution of the solid residue was subjected to column chromatography on a silica gel column. Elution with chloroform gave the fraction containing 2-BzO-$TPPH_2$. Further elution with chloroform/methanol (95/5 v/v) produced a green-brown fraction. The product was identified by means of electronic and ^{1}H NMR spectroscopy as (2-BzO-TPP)Mn^{III}Cl. The solution was evaporated to dryness, and the residue was recrystallized from dichloromethane/*n*-hexane (90% yield). UV−vis (CH_2Cl_2) λ_{max} (log ϵ): 373 (4.73), 400 (sh, 4.63), 479 (4.94), 580 (3.92), 619 nm (3.94).

The selectively deuterated complex was synthesized analogously from the corresponding deuterated 2-(benzoyloxy)porphyrin to produce (2-BzO-TPP-d_7)Mn^{III}Cl.

Insertions of manganese(III) into other β-substitued 5,10,15,20-teraphenylporphyrins were carried out in a similar manner.

[(2-O-TPP)Mn^{III}]$_3$. (2-BzO-TPP)Mn^{III}Cl (40 mg) was dissolved in 50 mL of ethanol, and the solution was heated under reflux. NaOH (3−5 pellets) was added to this solution. The color changed from dark red to brown. The heating was discontinued after 30 min. The reaction mixture was diluted with benzene and washed several times with aqueous NaOH and water. The organic layer was separated and dried with anhydrous magnesium sulfate. The solid material was filtered, and the filtrate was evaporated to dryness on the rotatory evaporator. The benzene solution of the solid residue was subjected to chromatography on a basic alumina column. Elution with benzene gave a brown fraction containing a solid that was recovered after the solvent was removed under vacuum. Recrystallization of this solid from

(44) (a) Chachaty, C.; Forchioni, A.; Ronfard-Haret, J. C. *Mol. Phys.* **1976**, *31*, 325. (b) Chachaty, C.; Rigny, P. *J. Chim. Phys.* **1982**, *79*, 203.
(45) Lisowski, L.; Latos-Grażyński, L.; Szterenberg, L. *Inorg. Chem.* **1992**, *31*, 1933.
(46) [(2-O-TPP)In^{III}]$_3$ presents the 3-H resonances at 2.58, 2.90, and 3.36 ppm (289 K). Wojaczyński, J.; Latos-Grażyński, L. *Unpublished results*.
(47) Lindsey, J. S.; Schreiman, I. C.; Hsu, H. C.; Kearney, P. C.; Marguerettaz, A. M. *J. Org. Chem.* **1987**, *52*, 827.
(48) Boersma, A. D.; Goff, H. M. *Inorg. Chem.* **1982**, *21*, 581.

benzene/*n*-hexane (50/50 v/v) produced [(2-O-TPP)Mn^{III}]$_3$ which precipitated as the black powder (60−70% yield).

UV−vis (CH_2Cl_2) λ_{max} (log ϵ, per porphyrin unit): 387 (4.58), 440 (sh, 4.47), 520 (sh, 4.31), ∼660 (sh). MS (LSIMS): $(m + 1)/z = 2047$ (0.6%), 1365 (13.3%), 683 (100%). Anal. Calcd for $C_{132}H_{81}N_{12}O_3Mn_3 \cdot C_6H_6$: C, 77.96; H, 4.12; N, 7.91. Found: C, 78.55; H, 4.68; N, 8.19.

[(2-O-TPP-d_6)Mn^{III}]$_3$ was synthesized following the procedure elaborated for [(2-O-TPP)Mn^{III}]$_3$.

(2-OH-TPP)Mn^{III}Cl. Hydrogen chloride in dichloromethane was added to the solution of [(2-O-TPP)Mn^{III}]$_3$ in dichloromethane. The solution was evaporated to dryness, and the solid residue was recrystallized from dichloromethane/*n*-hexane (50/50 v/v).

UV−vis (CH_2Cl_2) (log ϵ): 376 (4.79), 400 (sh), 480 (4.81), 581 (4.05), 615 nm (4.01).

Cleavage Procedures. Solutions of known concentration (2−3 mM in chloroform-*d* for ^{1}H NMR spectroscopy, 0.01−0.1 mM in dichloromethane for UV−vis spectroscopy) of the trimeric complex [(2-O-TPP)Mn^{III}]$_3$ were prepared. The respective solution of the cleaving reagent (HCl in chloroform-*d*, NaOH in methanol-d_4) was titrated by a syringe, and the progress of the reaction was monitored by ^{1}H NMR or UV−vis spectroscopy.

Instrumentation. ^{1}H NMR spectra were recorded on a Bruker AMX spectrometer operating in the quadrature mode at 300 MHz. A typical spectrum was collected over a 45 000 Hz spectral window with 16 K data points with 500−5000 transients for the experiment and a 50 ms prepulse delay. The free induction decay (FID) was apodized using exponential multiplication depending on the natural line width. This induced 5−80 Hz broadening. The residual ^{1}H NMR spectroscopic resonances of the deuterated solvents were used as a secondary reference. An inversion−recovery sequence was used to suppress the diamagnetic signals in the selected spectra. The deconvolution was carried out using standard Bruker software.

Absorption spectra were recorded on a Specord M-42 spectrometer and diode array Beckman 7500 spectrometer. Mass spectra were recorded on an AD-604 spectrometer using the liquid matrix secondary ion mass spectrometry technique and a primary beam of 8 keV Cs^+ ions. A Bruker 300 AMX spectrometer was used for magnetic susceptibility measurements by the Evans technique in solution using the peak of hexamethyldisiloxane as a reference.[41] Diamagnetic corrections were obtained by using published values for constitutive corrections for $TPPH_2$[49] and Pascal's constants.

Acknowledgment. Financial support of the State Committee for Scientific Research KBN (Grant 2 2651 92 03) is kindly acknowledged.

IC951663Y

(49) Eaton, S. S.; Eaton, G. R. *Inorg. Chem.* **1980**, *19*, 1095.